Duality, inverse problems and nonlinear problems in solid mechanics

A theoretical approach of strain localization within thin planar bands in porous ductile materials

Jean-Baptiste Leblond [a,*], Gérard Mottet [b]

[a] *Institut Jean-Le-Rond-d'Alembert, Université Paris VI, tour 65–55, 4, place Jussieu, 75252 Paris cedex 05, France*
[b] *ESI Group, Immeuble "Le Récamier", 70, rue Robert, 69458 Lyon cedex 06, France*

Abstract

Propagation of cracks in ductile materials is well known to occur through two possible mechanisms: coalescence of cavities and formation of shear bands ('void sheet mechanism'). The classical Gurson–Tvergaard–Needleman (GTN) homogenized model for such materials incorporates some phenomenological modelling of coalescence, but not of formation of shear bands assisted by the presence of microvoids, and this generates a number of shortcomings. In order to solve these difficulties, this paper presents a unified model of both coalescence and formation of shear bands in porous plastic solids, including the possible couplings between the two. Both phenomena are viewed as expressions of the same basic effect, namely strain localization within thin planar bands, the only difference being the mode of deformation. The model is first developed assuming a periodic distribution of cavities, then critically assessed through comparison with some micromechanical numerical simulations based on the same assumption, and finally extended to the case of a random distribution of voids. *To cite this article: J.-B. Leblond, G. Mottet, C. R. Mecanique 336 (2008).*
© 2007 Académie des sciences. Published by Elsevier Masson SAS. All rights reserved.

Résumé

Une approche théorique de la localisation de la déformation en minces couches planes dans les matériaux poreux ductiles. Il est bien connu que la propagation de fissures dans les matériaux poreux ductiles s'effectue suivant deux mécanismes possibles : la coalescence des cavités et la formation de bandes de cisaillement. Le modèle homogénéisé classique de Gurson–Tvergaard–Needleman (GTN) pour ces matériaux contient une modélisation phénoménologique de la coalescence, mais pas de la formation de bandes de cisaillement assistée par la présence de microcavités, et ceci induit certains inconvénients. Afin de résoudre ces difficultés, cet article propose un modèle unifié de la coalescence des vides et de la formation de bandes de cisaillement dans les solides plastiques poreux, incluant les couplages possibles entre les deux phénomènes. Ces derniers sont considérés comme deux manifestations d'un même effet fondamental, à savoir la localisation de la déformation en minces couches planes, la seule différence résidant dans le mode de déformation. Le modèle est d'abord développé en faisant l'hypothèse d'une distribution périodique de cavités, puis validé par comparaison avec des simulations numériques micromécaniques fondées sur la même hypothèse, et finalement étendu au cas d'une distribution aléatoire de vides. *Pour citer cet article : J.-B. Leblond, G. Mottet, C. R. Mecanique 336 (2008).*
© 2007 Académie des sciences. Published by Elsevier Masson SAS. All rights reserved.

---

* Corresponding author.
  E-mail addresses: leblond@lmm.jussieu.fr (J.-B. Leblond), gerard.mottet@esi-group.com (G. Mottet).

1. Introduction

There is ample experimental evidence that the final stage of ductile damage of metals, which leads to initiation and propagation of a macroscopic crack, can involve two distinct mechanisms. The first consists of coalescence of cavities and occurs in the case of highly triaxial stress fields, as encountered near the tip of mode I cracks. The second, so-called 'void sheet mechanism', consists of the formation of a shear band and occurs when the triaxiality is lower and at least one shear stress component is important. The two phenomena may be coupled: the presence of microvoids can assist the formation of a shear band, but conversely void growth may preferentially occur in the regions of localized strain.

Gurson's famous homogenized model [1] for plastic porous solids, in its original form, incorporated neither of the two mechanisms. The reason was that it was derived from approximate limit-analysis of some hollow plastic sphere (typical elementary cell in a porous ductile medium) subjected to conditions of homogeneous boundary strain rate, which precluded the localized velocity fields typical of coalescence of voids and deformation within shear bands. A very simple but efficient heuristic modelling of coalescence was therefore proposed by Tvergaard and Needleman [2]; the resulting extension of Gurson's model will be referred to as the GTN model in the sequel. The list of successful applications of the GTN model to problems of ductile rupture under highly triaxial stress fields is impressive.

However, the GTN model still does not incorporate any description of the formation of shear bands assisted by the presence of microvoids, nor of the possible enhanced growth of these voids in the regions of localized strain. This deficiency entails a number of drawbacks. One example pertains to the simulation of the so-called 'cup-cone' fracture of a smooth (un-notched) axisymmetric specimen. This problem was investigated by several authors, notably Tvergaard and Needleman themselves [2], Devaux et al. [3] and Besson et al. [4]. The very thorough study of the last authors has clearly shown that the final kink of the crack near the outer boundary of the specimen can indeed be reproduced by the GTN model, but *only when discarding Tvergaard and Needleman's modelling of coalescence*. (Coalescence, when accounted for, forces the crack to propagate along its original plane, perpendicularly to the axis of symmetry.) But eliminating coalescence from the model is an artificial solution, since it does occur in many cases. The problem with the model is not that it contains too many elements, but too few: what is lacking is a proper modelling of the possibility of the formation, assisted by the presence of microvoids, of a highly sheared region oriented at 45° from the original crack plane, along which the crack could propagate.

Another example relates to the simulation of ductile crack growth in mixed mode conditions. Experiments performed by Kyong Lak [5] for various values of the ratio K_{II}/K_I[1] have shown that even under conditions of predominant mode II, the kink angle of the crack is always much smaller than in brittle fracture, typically of the order of 20°. Attempts at reproducing such values through numerical simulations based on the GTN model [6] have all failed; the kink angle is always predicted to be much larger, of the order of 60° to 70° under conditions of predominant mode II. The most plausible explanation of the small kink angles actually observed is that the crack, when subjected to the high shear stresses typical of mode II, probably propagates along a shear band almost collinear to its initial direction. Again, the model lacks the basic ingredients to predict such a phenomenon.

The aim of this article is to solve these difficulties by proposing a new unified theoretical approach of both coalescence of voids and formation of shear bands in porous plastic solids, including the possible couplings between the two. The basic idea consists of considering coalescence of voids and formation of shear bands in porous materials, at some 'meso' (intermediary) scale, as two expressions of the same basic phenomenon, namely sudden concentration of the deformation within thin planar bands. The difference between the two, from this point of view, lies only in the mode of deformation, which consists of uniaxial extension in the direction perpendicular to the band in the case of coalescence, versus shear deformation in the case of a shear band. (It is worth noting, incidentally, that this point of view allows one to rationalize the fact that only two final, possibly combined failure mechanisms, namely coalescence of voids and formation of shear bands, have been observed in porous ductile materials. Indeed a defor-

---

[1] The quantities K_I and K_{II} here only represent conventional stress intensity factors.

mation field localized within a planar band is necessarily a combination of two modes only, pure extension and shear deformation.)

The approach is inspired from, and achieves a kind of synthesis between two previous works. The first one is Gologanu et al.'s model [7,8] of coalescence of voids in periodically voided solids. Just like many micromechanical numerical simulations initiated by Koplik and Needleman's pioneering work [9], Gologanu et al.'s analytical approach was based on consideration of some elementary cell in a porous periodic medium subjected to some axisymmetric loading with predominant axial stress. The main idea was to schematize this cell as a 'sandwich' made of three superposed planar layers, sound/porous/sound. The mechanical fields were considered as homogeneous in each layer, the outer sound ones obeying the von Mises criterion and the central porous one Gurson's criterion. The analytical solution of the problem evidenced two possible regimes, according to whether the outer layers were plastic like the central one or remained rigid. These two regimes were interpreted as representing the pre-coalescence and coalescence periods, respectively. During coalescence, the rigidity of the outer layers constrained the deformation mode of the central one to be a pure extension in the direction perpendicular to the layers.

Our second main source of inspiration is Drucker's [10] analysis of shear bands in porous materials. In this work, Drucker used limit-analysis to show that in such materials, a pure shear stress is more likely to promote localized deformation within thin planar bands containing cavities than homogeneous deformation.[2] The type of deformation he evidenced was very similar to that during the coalescence phase of Gologanu et al.'s [7,8] model, except that the deformation mode within the band of localized deformation was a shear strain instead of a uniaxial extension. In its original form, the argument applied only to distributions of voids for which planes containing a large number of void centers could be found: typically, periodic distributions. However Idiart and Ponte-Castaneda [11] recently showed that Drucker's result basically extends to random, macroscopically isotropic distributions of cavities. Their point was that the value of the overall yield stress under pure shear, as predicted by their "second order" homogenization theory, can be notably lower than that predicted by Gurson's model based on the consideration of regular (non-localized) velocity fields.

The paper is organized as follows:

- The model is first developed in Section 2 in the case of a periodic distribution of cavities. It is based on an extension of Gologanu et al.'s [7,8] treatment of coalescence, which considered only axisymmetric loadings, to more general ones including shear components. This extension remains tractable analytically because the basic approximation of homogeneity of the mechanical fields within each layer allows to reduce the initial complex boundary value problem to a set of simple (although non-linear) equations. The very construction of the model also ensures that it automatically incorporates Drucker's argument on shear bands.
- The model is then validated in Section 3 through comparison of its predictions with the results of some micromechanical numerical simulations, again in the case of a periodic distribution of voids. These simulations are basically similar to those of Koplik and Needleman [9] except that the loading now includes some shear component, which demands 3D computations and use of more complex, periodic boundary conditions. The simulations are found to fully confirm the model predictions.
- Section 4 is finally devoted to the extension of the model to the more physically significant case of a random distribution of cavities. The major problem here is to predict the orientation of the band of localized strain, which is no longer prescribed by the distribution of cavities. This is done by adopting an approach based on limit-analysis: the overall yield locus is calculated for every a priori possible orientation of the band, and that which yields the smallest overall yield stress is selected. The model also incorporates the effect of the anisotropy of the distribution of voids induced by the deformation.

It is hoped that the model developed, when coupled to the GTN model to describe both the early and late stages of ductile damage, will allow to reproduce the hitherto unexplained experimental results mentioned above.

---

[2] In fact Drucker considered only infinitesimally thin bands, that is discontinuous velocity fields. But his argument can readily be extended to bands of finite thickness, and applies as soon as the porosity within the band is larger than the mean porosity.

2. The model for a periodically voided solid

2.1. Generalities

Fig. 1 shows a 2D picture of some periodically voided, rigid-perfectly plastic material. In the initial state (Fig. 1(a)), the periodic lattice of void centers is cubic, so that the void spacing $2D$ is the same in the directions X, Y and Z. Each elementary cell of the lattice contains a spherical void of radius R, so that the porosity is $f_0 \equiv \pi R^3 / (6D^3)$. The macroscopic stress state $\boldsymbol{\Sigma}$ consists of some axisymmetric loading with predominant axial stress ($\Sigma_{xx} = \Sigma_{yy} < \Sigma_{zz}$) plus some additional shear component Σ_{xz}, the ratios

$$\rho_1 \equiv \frac{\Sigma_{xx}}{\Sigma_{zz}}; \qquad \rho_2 \equiv \frac{\Sigma_{xz}}{\Sigma_{zz}} \tag{1}$$

being constant in time. (This stress state is typical of conditions prevailing ahead of the tip of a crack loaded in mixed mode but is not fully general, and the conditions $\rho_1 = Cst.$ and $\rho_2 = Cst.$ are also restrictive. All these restrictions will be relaxed in Section 4.)

Because of this loading, in the deformed state, schematically represented in Fig. 1(b), the void spacing $2d_x = 2d_y$ in the directions x and y obtained by convective transport of the initial directions X and Y is smaller than the void spacing $2d_z$ in the direction z orthogonal to the plane xy. (Note that z does *not* represent the direction obtained by convective transport of the initial direction Z.) Any change of the void shape is disregarded so that the voids are still idealized as spherical, with radius r. The value of the porosity is now $f \equiv \pi r^3 / (6d_x^2 d_z)$.

Since in the deformed state, the voids are more closely packed in the horizontal directions than in the vertical one, strain localization is expected to occur within horizontal planar bands containing the voids, schematically delimited by dotted lines in Fig. 1(b). This geometrical and mechanical situation can be approximately represented by a superposition of alternately sound (s) and porous (p) planar layers, in which the stress and strain rate fields are considered as homogeneous and adequately described by von Mises's model and Gurson's model, respectively (Fig. 2(a)). In intuitive terms, this means performing some 'partial homogenization' of the heterogeneous fields at the 'meso' scale of the localization bands. The choice of an adequate value of the thickness $2h$ of the porous layers is of course a central question but is postponed for the moment. The natural invariance of the problem in the directions x and y implies that one may concentrate on a rectangular parallelepiped of sides $2d_x = 2d_y$ and $2d_z$ consisting of one central porous layer (containing a single void) surrounded by two sound ones (Fig. 2(b)).
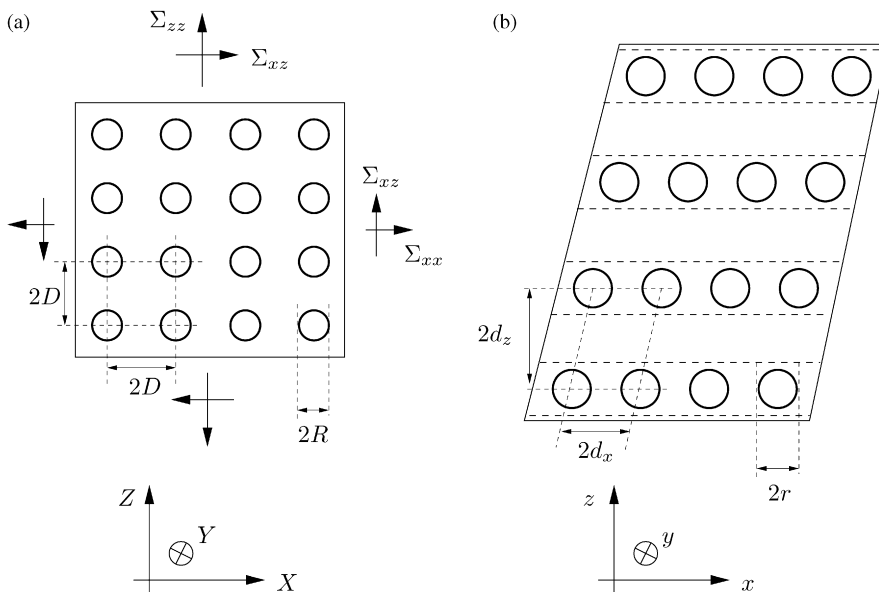

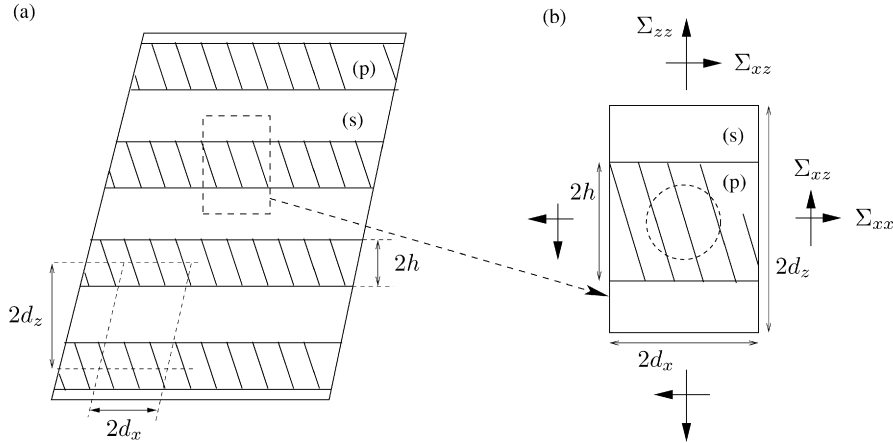Fig. 1. Deformation of a periodically voided material.

Fig. 2. The sandwich model.

Quantities pertaining to the sound and porous layers will be denoted with upper $^{(s)}$ and $^{(p)}$ indices, respectively. With this notation, the definition of macroscopic stresses and the continuity of the stress vector across the horizontal interfaces imply that the components of the stress tensors $\mathbf{\Sigma}^{(s)}$, $\mathbf{\Sigma}^{(p)}$ in the sound and porous layers are related to those of the overall stress tensor $\mathbf{\Sigma}$ through the following formulae:

$$\begin{cases} (1-c)\Sigma_{xx}^{(s)} + c\Sigma_{xx}^{(p)} = \Sigma_{xx} \\ \Sigma_{zz}^{(s)} = \Sigma_{zz}^{(p)} = \Sigma_{zz} \\ \Sigma_{xz}^{(s)} = \Sigma_{xz}^{(p)} = \Sigma_{xz} \end{cases} \tag{2}$$

where

$$c \equiv \frac{h}{d_z} \tag{3}$$

denotes the volume fraction of the central layer. Also, the definition of the macroscopic strain rate and the continuity of the tangential strain rate across the interfaces imply that the components of the strain rate tensors $\mathbf{D}^{(s)}$, $\mathbf{D}^{(p)}$ in the sound and porous layers are related to those of the overall strain rate tensor $\mathbf{D}$ through the relations

$$\begin{cases} D_{xx}^{(s)} = D_{xx}^{(p)} = D_{xx} \\ (1-c)D_{zz}^{(s)} + cD_{zz}^{(p)} = D_{zz} \\ (1-c)D_{xz}^{(s)} + cD_{xz}^{(p)} = D_{xz} \end{cases} \tag{4}$$

2.2. Version of the model based on homogenization (H model)

The simplest version of the model, which will be denoted symbolically with a letter H, is obtained by adopting the 'homogenized' picture of the heterogeneous porous cell schematized in Fig. 2 throughout the entire mechanical history. This was exactly the approach adopted by Gologanu et al. [7,8] to describe coalescence only. The task reduces to solving a simple plasticity problem for a sandwich made of homogeneous layers. Two cases must be distinguished since the outer, stronger layers may be either plastic or rigid. (The central weaker layer is necessarily plastic.)

2.2.1. Case of plastic outer layers (pre-localization phase)

In this case the stresses can be determined independently of the velocity field. Indeed the yield criterion in the sound layers yields

$$\left(S_{zz} - S_{xx}^{(s)}\right)^2 + 3S_{xz}^2 = 1 \quad \Rightarrow \quad S_{xx}^{(s)} = S_{zz} - \sqrt{1 - 3S_{xz}^2} \tag{5}$$

where 'normalized' stresses obtained through division by the yield stress and denoted by the letter S are used. It then follows from Eq. $(2)_1$ that

$$S_{xx}^{(p)} = \frac{1}{c}\big[S_{xx} - (1-c)S_{xx}^{(s)}\big] = \frac{1}{c}\big[S_{xx} - (1-c)\big(S_{zz} - \sqrt{1-3S_{xz}^2}\big)\big] \tag{6}$$

Also, Gurson's criterion in the porous layer reads

$$\big(S_{zz} - S_{xx}^{(p)}\big)^2 + 3S_{xz}^2 + 2p\cosh\left(S_{xx}^{(p)} + \frac{S_{zz}}{2}\right) - 1 - p^2 = 0, \quad p \equiv qf^{(p)}, \ f^{(p)} \equiv \frac{f}{c} \tag{7}$$

where q denotes Tvergaard's [12] parameter and $f^{(p)}$ the porosity within the porous layer. Combining Eqs. (6) and (7), one gets an equation on the sole overall stresses S_{xx}, S_{zz} and S_{xz}. Since S_{xx} and S_{xz} are related to S_{zz} by Eqs. (1) where ρ_1 and ρ_2 are assumed to be known, this is in fact an equation on the sole unknown S_{zz}, which can be solved at least numerically. The values of the other stress components then follow from Eqs. (1), (5) and (6). Once all stresses are known, the flow rules associated to von Mises's criterion in the sound layers and Gurson's criterion in the porous one yield the components of the strain rates in these layers (up to some arbitrary multiplicative constant because of the hypothesis of perfect plasticity):

$$\begin{cases} \dfrac{D_{zz}^{(s)}}{D_{xx}} = -2, \qquad \dfrac{D_{xz}^{(s)}}{D_{xx}} = -\dfrac{3S_{xz}}{S_{zz} - S_{xx}^{(s)}} \\[3mm] \dfrac{D_{zz}^{(p)}}{D_{xx}} = \dfrac{2(S_{zz} - S_{xx}^{(p)}) + p\sinh(S_{xx}^{(p)} + S_{zz}/2)}{-S_{zz} + S_{xx}^{(p)} + p\sinh(S_{xx}^{(p)} + S_{zz}/2)}, \qquad \dfrac{D_{xz}^{(p)}}{D_{xx}} = \dfrac{3S_{xz}}{-S_{zz} + S_{xx}^{(p)} + p\sinh(S_{xx}^{(p)} + S_{zz}/2)} \end{cases} \tag{8}$$

The components of the overall strain rate then follow from Eqs. (4). Finally, the evolutions of the internal parameters d_x, d_z and f are given by the following equations, the last of which is a consequence of matrix incompressibility:

$$\dot{d}_x = D_{xx}d_x, \qquad \dot{d}_z = D_{zz}d_z, \qquad \dot{f} = (1-f)(2D_{xx} + D_{zz}) \tag{9}$$

(The dimensions of the cell are needed to evaluate the volume fraction c of the porous layer through Eq. (3), once a value has been ascribed to the thickness $2h$ of this layer.)

2.2.2. Case of rigid outer layers (post-localization phase)

The pre-localization phase lasts as long as the horizontal strain rate D_{xx} remains nonzero. When it becomes zero, the sound layers become rigid, so that it remains zero afterwards. Eq. (5) then no longer applies, but the condition $D_{xx} = 0$ implies, by the flow rule associated to Gurson's criterion in the porous layer, that

$$-S_{zz} + S_{xx}^{(p)} + p\sinh\left(S_{xx}^{(p)} + \frac{S_{zz}}{2}\right) = 0 \tag{10}$$

Combination of this equation and Gurson's criterion (7) yields the following second-order equation on the unknown $\cosh(S_{xx}^{(p)} + S_{zz}/2)$:

$$p^2\cosh^2\left(S_{xx}^{(p)} + \frac{S_{zz}}{2}\right) + 2p\cosh\left(S_{xx}^{(p)} + \frac{S_{zz}}{2}\right) - 1 - 2p^2 + 3S_{xz}^2 = 0 \tag{11}$$

the solution of which is

$$\cosh\left(S_{xx}^{(p)} + \frac{S_{zz}}{2}\right) = -\frac{1}{p} + \sqrt{2 + \frac{2 - 3S_{xz}^2}{p^2}} \tag{12}$$

(The other solution can safely be discarded because it is smaller than unity). Combination of Eqs. (10) and (12) then yields

$$\begin{cases} S_{zz} = 2(\gamma + p\sinh\gamma)/3, \\ S_{xx}^{(p)} = (2\gamma - p\sinh\gamma)/3, \end{cases} \quad \gamma \equiv \arg\cosh\left(-\frac{1}{p} + \sqrt{2 + \frac{2 - 3S_{xz}^2}{p^2}}\right) \tag{13}$$

Eq. $(13)_1$, where γ is given by $(13)_3$ and S_{xz} is related to S_{zz} through $(1)_2$ in which ρ_2 is assumed to be known, is an equation on the sole unknown S_{zz}, which again can be solved at least numerically. The other stress components

then follow from Eqs. (1), (2) and (13)$_2$. All strain rate components are zero in the sound layers, and the ratio of the nonzero strain rate components in the porous layer is given by

$$\frac{D_{xz}^{(p)}}{D_{zz}^{(p)}} = \frac{S_{xz}}{S_{zz} - S_{xx}^{(p)}} \tag{14}$$

(where use has been made of Eq. (10)). The components of the overall strain rate are then deduced from Eqs. (4). Finally the evolutions of the internal parameters d_x, d_z and f are given by the same Eqs. (9) as above.

2.3. Version of the model based on limit-analysis (LA model)

Another, slightly different version of the model, symbolically denoted with the letters LA, is based on limit-analysis. Although this version is somewhat less natural than the previous one, it is better fit for the necessary extension to random distributions of cavities, as will be seen in Section 4. The use of limit-analysis makes it in fact closer in spirit to the coalescence model of Perrin [13], and also those of Zhang and Niemi [14], Pardoen and Hutchinson [15] and Benzerga [16] based on the earlier works of Thomason [17,18], than to that of Gologanu et al. [8]. (Note, however, that Gologanu also proposed in his thesis [1] a variant of his model based on limit-analysis.)

The main difference with the first version of the model is that the idealized representation of the elementary cell as a sandwich made of homogeneous layers is adopted *only during the post-localization phase*. The idea is to distinguish between two kinds of trial velocity fields. The first is non-localized, and the corresponding estimate of the overall yield stress is assumed to be given by Gurson's criterion applied at the scale of the entire representative cell. The second velocity field is localized within a horizontal band containing the void, and the corresponding estimate of the overall yield stress is assumed to be given by the sandwich model. The velocity field which actually prevails is considered to be, by the theory of limit-analysis, that which yields the lower estimate of the overall yield stress.

Thus, during the pre-localization phase, the overall stresses are to be deduced from Eqs. (7), with S_{xx} and f instead of $S_{xx}^{(p)}$ and $f^{(p)}$. The components of the overall strain rate are given by Eqs. (8)$_3$ and (8)$_4$, with D_{zz}, D_{xz}, S_{xx} and f instead of $D_{zz}^{(p)}$, $D_{xz}^{(p)}$, $S_{xx}^{(p)}$ and $f^{(p)}$. On the other hand the equations pertaining to the post-localization phase are unchanged.

It is worth noting that the condition marking the transition between the two phases in this new version of the model, namely equality of the overall stress components obtained from the equations corresponding to the pre- and post-localization phases, is different from that in the first version of the model, namely vanishing of the component D_{xx} of the overall strain rate. The new condition is unavoidable since it is the only one which ensures continuous variation of the overall stresses at the transition between the two phases.

2.4. Connection with Drucker's argument on shear bands in porous solids

We shall now explain how the LA model incorporates Drucker's argument [10] on the formation of shear band in porous plastic materials. This argument in fact merely corresponds to what the model says in the special case of a pure shear loading.

Drucker's point was based on two observations. First, the estimate of the overall yield stress under pure shear (normalized by the yield stress of the sound material) resulting from a uniform trial strain rate field is $(1 - f)/\sqrt{3}$, where f denotes the overall porosity. Second, the estimate resulting from a trial strain rate field localized within a band is $(1 - f^{(p)})/\sqrt{3}$, where $f^{(p)}$ denotes the porosity within this band. Since $f^{(p)}$ is larger than f, the second estimate is lower than the first one, and therefore better by the theory of limit-analysis. This means that in pure shear, the material prefers to deform through formation of a shear band rather than uniformly.

Now the LA model is based on exactly the same comparison of overall yield stresses, and the estimates of the overall yield stress under pure shear it compares are exactly the same. Indeed in the pre-localization phase, Gurson's criterion, applied at the scale of the entire elementary cell (Eq. (7) with S_{xx} and f instead of $S_{xx}^{(p)}$ and $f^{(p)}$), yields, for

$S_{xx} = S_{zz} = 0$ and $q = 1^3$: $|S_{xz}| = (1 - f)/\sqrt{3}$. Also, in the post-localization phase, Eq. (11) yields, for $S_{xx}^{(p)} = S_{zz} = 0$ and $q = 1$: $|S_{xz}| = (1 - f^{(p)})/\sqrt{3}$. This establishes the equivalence announced.

3. Numerical validation

3.1. Presentation of the simulations

The model developed will now be validated through comparison of its predictions with the results of some micromechanical numerical simulations. These simulations are quite analogous in principle to those of Koplik and Needleman [9] (and many later ones) of coalescence in periodically voided materials, but more complex in detail. The major novelty lies in the introduction of some extra macroscopic shear stress.[4] This introduction makes Koplik and Needleman's hypothesis of axisymmetry inapplicable, so that a fully 3D mesh becomes necessary. The elementary cell considered in this work is, in the initial configuration, a cube containing a spherical void. This cell is subjected to the same kind of macroscopic stress state as in Section 2, consisting of some axisymmetric loading with predominant axial stress ($\Sigma_{xx} = \Sigma_{yy} < \Sigma_{zz}$) plus some shear component Σ_{xz}. The ratios ρ_1, ρ_2 defined by Eq. (1) are kept constant throughout the entire mechanical history.

This type of loading generates two complications. The first pertains to boundary conditions. The presence of some macroscopic shear stress component forbids one to make the usual hypothesis that the initially planar faces of the cell remain planar. Conditions of homogeneous boundary strain rate are no more applicable, because they would preclude localized velocity fields. The only possibility thus left is to adopt rigorous periodic boundary conditions, as defined by Suquet [20]. This means that the velocity field is taken in the form

$$\mathbf{v}(\mathbf{x}) = \mathbf{D} \cdot \mathbf{x} + \boldsymbol{\Omega} \cdot \mathbf{x} + \tilde{\mathbf{v}}(\mathbf{x}) \tag{15}$$

on the outer boundary, where $\boldsymbol{\Omega}$ (the macroscopic rotation rate) is an antisymmetric tensor and $\tilde{\mathbf{v}}(\mathbf{x})$ a periodic velocity field. In practice, the value of $\boldsymbol{\Omega}$ is chosen so as to ensure absence of rotation of the horizontal plane xy (see Figs. 1(a) and (b)). Also, the unknown periodic velocity field $\tilde{\mathbf{v}}(\mathbf{x})$ is eliminated by writing Eq. (15) at two points in correspondence through periodicity, and taking the difference. This yields a relation between the velocities at these two points, which is enforced by connecting them through some special 1D element with a very high stiffness. The procedure is repeated for all couples of points in correspondence through periodicity.

Another difficulty is that what is prescribed on the boundary is the velocity field, whereas what one in fact wants to control is the overall stresses, through the imposed values of the ratios ρ_1 and ρ_2. This control is achieved by adjusting the values of the components of the macroscopic strain rate $\mathbf{D}$ by some Newton method. In practice, a 'higher level' program written in a special language fit for such applications runs the FE calculation, examines the results, computes the overall stresses through integration, performs a Newton iteration on the components of $\mathbf{D}$, runs a new FE calculation, and so on. The derivatives required by Newton's method are evaluated through numerical differentiation, that is by performing extra FE calculations with slightly perturbed values of the components of $\mathbf{D}$.

Only one value of the initial porosity, $f_0 = 0.02$, is considered. This admittedly rather high value is adopted in order to avoid having to considerably refine the mesh around a very small void. The material is elastic-perfectly plastic and obeys von Mises's criterion and the associated flow rule. (The introduction of elasticity is necessary for numerical reasons, but its influence is insignificant, the elastic strain being always much smaller than the plastic strain.) The values of Young's modulus, Poisson's ratio and the yield stress in simple tension are 200 000 MPa, 0.3 and 450 MPa respectively. Several values of the parameters[5]

$$T \equiv \frac{\Sigma_m}{\Sigma_{\text{eq}}}; \qquad S \equiv \frac{\sqrt{3}|\Sigma_{xz}|}{\Sigma_{\text{eq}}} \tag{16}$$

---

[3] Tvergaard's [12] introduction of the parameter q in Gurson's model was equivalent to artificially modifying the porosity. Since Drucker's argument did not involve any such artificial adjustment, it can be recovered only by setting $q = 1$.

[4] It is worth noting that similar simulations involving such a shear stress were performed very recently by Pardoen and Scheyvaerts [19], but these authors concentrated on void shape effects and especially on the rotation of non-spherical voids under shear loadings, rather than on strain localization.

[5] T is the usual triaxiality, and S (which lies in the interval [0, 1]) characterizes the importance of the shear stress component.

(where Σ_m denotes the mean macroscopic stress and Σ_{eq} the equivalent von Mises macroscopic stress) are considered, namely $T = 1$ and 2 and $S = 0, 0.25, 0.5$ and 0.75, which makes a total of 8 calculations.

All computations are performed using the *Large Strain Plasticity* option of the SYSTUS® FE code developed by ESI Group.

3.2. Parameters of the analytical model used in the comparison

The value of Tvergaard's [12] parameter q used in the comparison with the analytical model is 1.3. This is a slightly smaller value than that of 1.5 recommended by Tvergaard himself from micromechanical numerical simulations, and the almost identical value of $4/e \approx 1.47$ derived by Perrin and Leblond [21] from some theoretical differential scheme. The value adopted is logical since q is known to be a decreasing function of the porosity [21], and the initial porosity of 0.02 considered here is quite high.

It also becomes necessary to ascribe some precise value to the thickness $2h$ of the homogeneous porous layer which schematizes the band of localized strain in the model. It has been argued by Benzerga [16] that the most logical choice would be $h \equiv r$ (the radius of the void), since numerical simulations of coalescence have shown that the band extends up and down to, but not beyond, the poles of the void. Unfortunately numerical experience shows that the agreement between numerical and theoretical results obtained with this choice is mediocre. The basic reason seems to be that the central layer of the sandwich (see Fig. 2(b)) is then quite flat, and Gurson's model applies badly to elementary volumes of such shapes. The choice made here,

$$h \equiv d_x \tag{17}$$

is identical to that made by Perrin [21] in his coalescence model and yields much better results. The probable reason is that with this choice, the length, width and height of the central layer are equal, so that its shape is cubic and as close as possible to the spherical shape of the representative cell considered by Gurson.

It is clear that Eq. (17) is not fully satisfactory. It must be stressed, however, that this shortcoming of the model is not fundamental but merely tied to the approximation made when describing the behavior of the band of localized strain through Gurson's homogenized model. Another, probably more theoretically satisfactory possibility, would be to describe it through some suitable extension of Thomason's [17,18] treatment of coalescence (based on detailed analysis of the microscopic velocity field around the void) to non-axisymmetric loadings. It is not clear, however, that such an extension could be achieved, considering the complexity of Thomason's analysis in the simpler case he considered.

3.3. Results

For space reasons, we shall only present a small selection of the results obtained. Figs. 3 and 4 first show a 3D perspective of the deformed mesh somewhat after the onset of strain localization, for $(T, S) = (1, 0.5)$ and $(2, 0.75)$ respectively. In fact the cell is symmetric about the xz plane, so that only half of it is meshed; the face shown in these figures is precisely the plane of symmetry which cuts the cell in two, so that the limit of the crater representing half of the void is clearly visible (as a red line). Also, the colors represent the value of the microscopic equivalent cumulated plastic strain on the surface which is seen; clearly, this cumulated strain is maximum on the surface of the void. But the main feature illustrated in these figures is the concentration of the deformation in the region extending roughly between two horizontal planes containing the poles of the void. The deformation mode in this zone consists of both vertical extension and shear in Fig. 3, but almost exclusively of shear in Fig. 4.

The next figures provide results for the sole case $(T, S) = (1, 0.5)$. In all of them, FE results are represented in red, predictions of the H model in green and predictions of the LA model in blue. Fig. 5 shows the overall equivalent stress (normalized by the yield stress of the sound material) versus the overall equivalent cumulated strain E_{eq}, and Figs. 6, 7 and 8 display the evolutions of the porosity and the overall strains E_{xx} and E_{xz} (that is, the integrals of D_{xx} and D_{xz} in time) in a similar way.[6] Strain localization is marked by a large decrease of the overall stress in Fig. 5, a large increase of the porosity in Fig. 6, and a stabilization of the E_{xx} strain in Fig. 7. Both models yield satisfactory

---

[6] The evolution of E_{zz} is not shown because it is rather trivial, this strain component being almost proportional to E_{eq}.

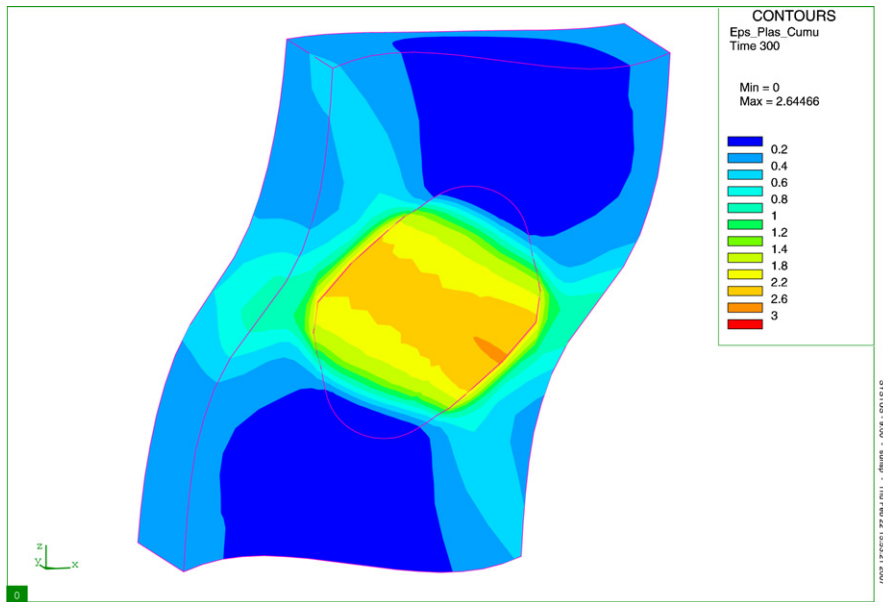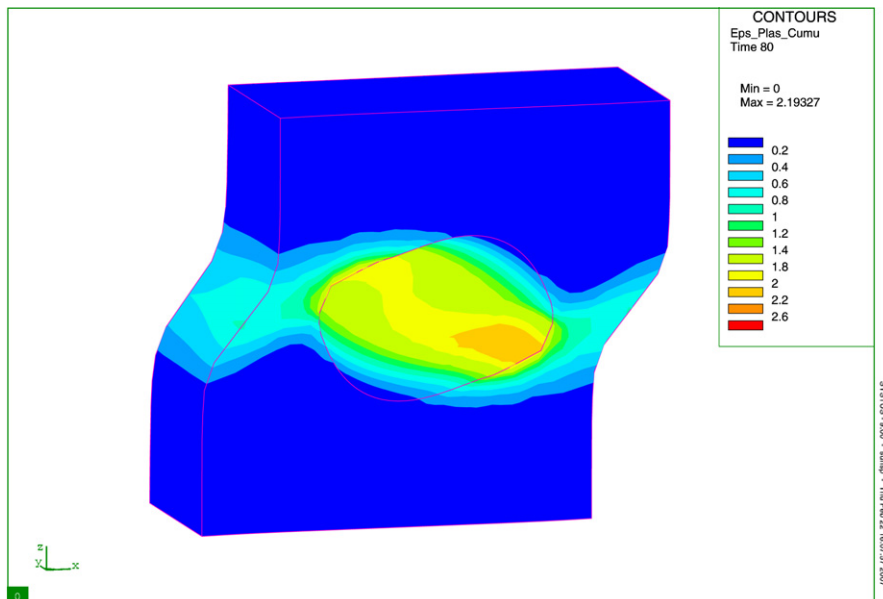Fig. 3. Deformed mesh—$T = 1$, $S = 0.5$ (the displacements are not magnified).

Fig. 4. Deformed mesh—$T = 2$, $S = 0.75$ (the displacements are not magnified).

predictions of the numerical results. One may note incidentally that with the LA model, the transition between the pre- and post-localization phases is marked, on the curves representing the overall stress, the porosity and the E_{xx} strain, by angular points which appear neither with the H model nor in the FE results. But this does not prevent the LA model from capturing the overall evolutions of all quantities quite well.
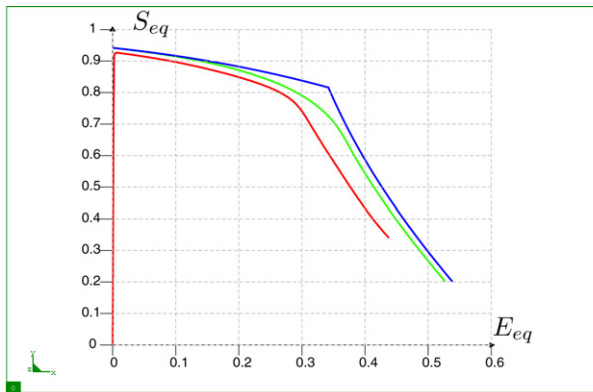
Fig. 5. Evolution of the macroscopic equivalent stress—$T = 1$, $S = 0.5$. FE results in red, H model in green, LA model in blue.
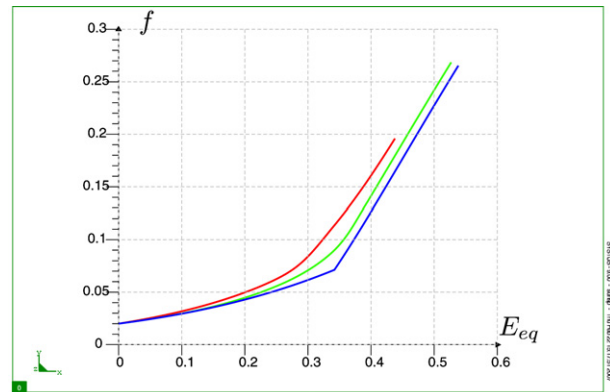

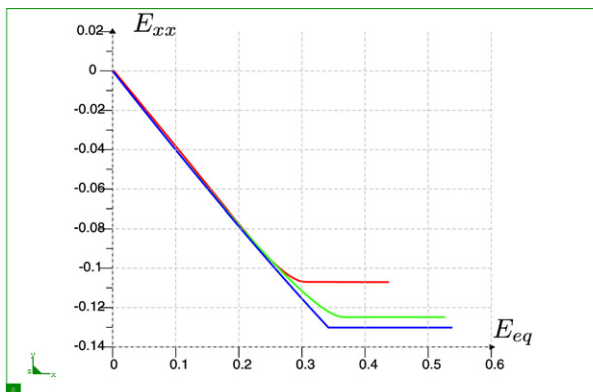Fig. 6. Evolution of the porosity—$T = 1$, $S = 0.5$. FE results in red, H model in green, LA model in blue.

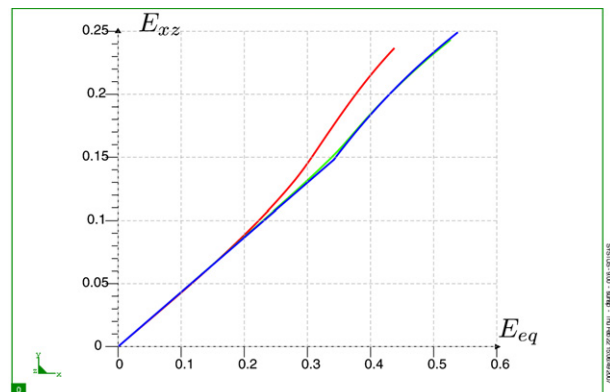Fig. 7. Evolution of the horizontal strain—$T = 1$, $S = 0.5$. FE results in red, H model in green, LA model in blue.

Fig. 8. Evolution of the shear strain—$T = 1$, $S = 0.5$. FE results in red, H model in green, LA model in blue.

4. The model for a randomly voided solid

4.1. Generalities

We shall finally extend the model of Section 2 to random distributions of cavities. For such distributions, the deformation may still concentrate within thin, approximately planar bands containing a large number of voids, and one may still adopt the schematic picture of a sandwich made of homogeneous, alternately sound and porous layers. What is new, however, is that the orientation of the bands of localized strain is no longer fixed a priori by the distribution of voids like in the periodic case. It thus becomes necessary to consider all possible orientations and determine the actual one through some suitable procedure.

We shall use the LA model rather than the H model. The reason is that in the latter model, the schematization of the elementary cell as a sandwich is used throughout the entire mechanical history, which demands choosing the orientation of the sandwich right from the beginning. This does not raise any problem if the distribution of voids is periodic, but extending the approach to random distributions would be hampered by the difficulty, for such distributions, of making such a choice *prior to strain localization*.

The problems to be solved are threefold. First, one must calculate, for every orientation of the normal vector **n** to the possible band of localized strain, the volume fraction c_n of this band within the elementary volume element, because this fraction will appear in the expression of the macroscopic yield criterion pertaining to the post-localization phase. Second, one must extend the expression of this criterion found in Section 2.2, which applied only to special

loadings, to fully general ones. Third, one must define a procedure of selection of the actual orientation of the band among all those a priori possible.

4.2. Calculation of the volume fraction of the band of localized strain

The calculation of the volume fraction c_n of the band of localized strain within the elementary cell, as a function of the gradient of the macroscopic transformation $\mathbf{F}$, is based on the following heuristic extension of Eqs. (3) and (17):

$$c_n \equiv \frac{d_{xy}}{d_z} \tag{18}$$

where $2d_{xy}$ and $2d_z$ denote the mean void spacings in the plane xy of the band and in the perpendicular direction z. The exact calculation of d_{xy} and d_z is a difficult problem because, as noted by Perrin [13], the evolution of these quantities in time depends on the 'degree of order' of the initial distribution of cavities.[7] We shall adopt here instead the simplistic, but reasonable hypothesis that the value of d_{xy} is governed by the evolution of some elementary area within the plane of the band, and that of d_z by the evolution of some elementary length in the perpendicular direction.

More specifically, let the distribution of voids be assumed to be initially macroscopically isotropic, and let $2D$ denote the initial mean void spacing. Consider, in the initial configuration, a cube of side $2D$ and volume $\Omega \equiv 8D^3$, select two opposite faces on this cube (parallel to the plane XY), denote by $\mathbf{N}$ the unit normal vector to these faces (parallel to the direction Z), and by $A \equiv 4D^2$ their common area. In the deformed configuration, this cube becomes an oblique parallelepiped of volume ω, the area of the selected faces (parallel to the plane xy) becomes $a \equiv 4d_{xy}^2$ by the very definition of d_{xy}, the unit normal vector to these faces (parallel to the direction z) becomes $\mathbf{n}$, and the height of the parallelepiped becomes $2d_z$. (One may again refer here to Fig. 1 although the distribution of cavities is no longer periodic. Again, note that the direction z is *not* obtained by convective transport of the initial direction Z; similarly, although the planes XY and xy *are* in correspondence though convective transport, the same is generally not true of the directions X and x, Y and y.)

The area vectors $\mathbf{A} \equiv A\mathbf{N}$ and $\mathbf{a} \equiv a\mathbf{n}$ are connected through the classical relation $\mathbf{A} = J^{-1}\mathbf{F}^T . \mathbf{a}$, where J denotes the determinant of $\mathbf{F}$. Therefore the relation between the areas A and a reads

$$A^2 = \mathbf{A} . \mathbf{A} = J^{-2}\mathbf{a} . \mathbf{F} . \mathbf{F}^T . \mathbf{a} \quad \Rightarrow \quad \frac{A}{a} = J^{-1}\sqrt{\mathbf{n} . \mathbf{F} . \mathbf{F}^T . \mathbf{n}} \tag{19}$$

Also,

$$\omega = 2ad_z = J\Omega = 2JAD \quad \Rightarrow \quad \frac{d_z}{D} = J\frac{A}{a} \tag{20}$$

Combination of Eqs. (18), (19) and (20) yields

$$c_n = \frac{d_{xy}}{D}\frac{D}{d_z} = \sqrt{\frac{a}{A}}\frac{D}{d_z} = J^{-1}\left(\frac{a}{A}\right)^{3/2} = \sqrt{J}\left(\mathbf{n} . \mathbf{F} . \mathbf{F}^T . \mathbf{n}\right)^{-3/4} \tag{21}$$

which is the result looked for. The value of c_n provided by Eq. (21) may be larger than 1 in some cases, and should then of course be replaced by unity.

4.3. Yield criterion and flow rule for strain localized within a band

In order to find the macroscopic yield criterion pertaining to strain localization within a postulated band of normal $\mathbf{n}$, one just needs to extend the treatment of Section 2.2 to arbitrary overall stress states. This is easily done by choosing arbitrary directions x, y within the plane of the band, and combining Gurson's criterion in this band with the conditions $D_{xx} = D_{yy} = D_{xy} = 0$ expressing the rigidity of the sound layers. The result reads

$$N_n = \pm\frac{2}{3}(\gamma_n + p_n \sinh \gamma_n), \quad p_n \equiv q\frac{f}{c_n}, \quad \gamma_n \equiv \arg\cosh\left(-\frac{1}{p_n} + \sqrt{2 + \frac{2 - 3\|\mathbf{T}_n\|^2}{p_n^2}}\right) \tag{22}$$

---

[7] The difficulty arises from the fact that the nearest neighbors of a given void may change in time.

where N_n and $\mathbf{T}_n$ are the normal and tangential components of the normalized stress vector $\mathbf{S} \cdot \mathbf{n}$ exerted on the band:

$$N_n \equiv \mathbf{n} \cdot \mathbf{S} \cdot \mathbf{n}, \qquad \mathbf{T}_n \equiv \mathbf{S} \cdot \mathbf{n} - N_n \mathbf{n} \tag{23}$$

and $\|\mathbf{T}_n\|$ is the Euclidian norm of $\mathbf{T}_n$.

One may note that the criterion (22) is the same (except for the '$\pm$') as that found in Section 2.2, even though the loading is more general. It is independent in particular of the in-plane (normalized) stress components S_{xx}, S_{yy}, S_{xy}. This property is tied to the peculiar deformation mode of the band which consists only of pure extension ($D_{zz} \neq 0$) plus shear ($D_{xz} \neq 0$, $D_{yz} \neq 0$). Indeed the criterion (22) basically arises from the fundamental inequality of limit-analysis, $\mathbf{\Sigma} : \mathbf{D} \leqslant \Pi(\mathbf{D})$ where $\Pi(\mathbf{D})$ denotes the overall plastic dissipation; but this inequality cannot possibly put any restriction on the stress components $\Sigma_{xx}, \Sigma_{yy}, \Sigma_{xy}$ since $D_{xx} = D_{yy} = D_{xy} = 0$ for the trial velocity fields considered.

It is also easy to derive the macroscopic flow rule. The direction x being chosen parallel to the tangential component $\mathbf{T}_n$ of the stress vector, the result is analogous to that found in Section 2.2 (Eq. (14)). It can be checked that this overall flow rule obeys the normality property with respect to the overall criterion (22). This property is not fortuitous but arises from a well-known theorem of limit-analysis.

4.4. Choice of the orientation of the bands of localized strain

The model proposed belongs to the category of multi-surface plasticity models. The yield surfaces include that of Gurson for the pre-localization phase, plus those pertaining to strain localization within bands of all possible orientations. (There are in fact infinitely many such surfaces.)

According to the general theory of limit-analysis, the yield surface to be used must be chosen by the following procedure. Choose and fix the values of the ratios $R_{ij} \equiv \Sigma_{ij}/\|\mathbf{\Sigma}\|$ where $\|\mathbf{\Sigma}\|$ denotes the Euclidian norm of $\mathbf{\Sigma}$. On each yield surface, determine that point $\mathbf{\Sigma}$ which satisfies the conditions $\Sigma_{ij}/\|\mathbf{\Sigma}\| = R_{ij}$. The surface to be selected is then that which yields the smallest value of $\|\mathbf{\Sigma}\|$. It may be that of Gurson or that corresponding to strain localization within a band of specific orientation. Once this choice is made, the flow rule to be considered is that associated to the yield criterion *via* the normality property.

The complexity of the minimization problem unfortunately forbids to solve it by analytical methods. It will therefore be necessary to perform the minimization numerically, using a discretization of the unit sphere spanned by the normal vector $\mathbf{n}$ to the possible band of localization. The future numerical implementation of the model in some FE code can be sketched as follows. At each Gauss point of the structure and for every time-step $[t, t + \Delta t]$, the first step will consist of determining the yield surface to be used. It will probably be necessary here to use the explicit estimates of the ratios R_{ij} provided by their values at time t. The points $\mathbf{\Sigma}$ respecting these ratios will be determined on a large but finite number of yield surfaces obtained through discretization of the unit sphere, plus Gurson's surface. That surface corresponding to the smallest value of $\|\mathbf{\Sigma}\|$ will be selected. The second, more classical step will then consist of 'projecting' the elastic predictor onto the yield surface, using Nguyen's [22] well-known implicit algorithm.

References

[1] A.L. Gurson, Continuum theory of ductile rupture by void nucleation and growth: Part I—Yield criteria and flow rules for porous ductile media, ASME J. Engrg. Mater. Technol. 99 (1977) 2–15.

[2] V. Tvergaard, A. Needleman, Analysis of cup-cone fracture in a round tensile bar, Acta Metallurgica 32 (1984) 157–169.

[3] J. Devaux, J.B. Leblond, G. Mottet, G. Perrin, Some new applications of damage models for ductile metals, in: Application of Local Fracture/Damage Models to Engineering Problems, Proceedings of the 1992 ASME Summer Mechanics Meeting, Tempe (USA), American Society of Mechanical Engineers.

[4] J. Besson, D. Steglich, W. Brocks, Modelling of crack growth in round bars and plane strain specimens, Int. J. Solids Structures 38 (2001) 8259–8284.

[5] J. Kyong Lak, Rupture en mode mixte I + II de l'acier inoxydable austénitique 316L, PhD Thesis, Ecole Centrale de Paris, France, 1993.

[6] J. Devaux, Etude de la rupture en mode mixte, action 2004—Application à la rupture d'un barreau de flexion 4 points, Note Interne ESI Group n° F/LE/04.5877/A, 2004.

[7] M. Gologanu, Etude de quelques problèmes de rupture ductile des métaux, PhD thesis, Université Pierre et Marie Curie (Paris VI), France, 1997.

[8] M. Gologanu, J.B. Leblond, G. Perrin, J. Devaux, Theoretical models for void coalescence in porous ductile solids—I: Coalescence "in layers", Int. J. Solids Structures 38 (2001) 5581–5594.

[9] J. Koplik, A. Needleman, Void growth and coalescence in porous plastic solids, Int. J. Solids Structures 24 (1988) 835–853.

[10] D.C. Drucker, The continuum theory of plasticity on the macroscale and the microscale, J. Materials 1 (1966) 873–910.

[11] M. Idiart, P. Ponte-Castaneda, Second order estimates for nonlinear isotropic composites with spherical pores and rigid particles, C. R. Mécanique 333 (2005) 147–154.

[12] V. Tvergaard, Influence of voids on shear band instabilities under plane strain conditions, Int. J. Fracture 17 (1981) 389–407.

[13] G. Perrin, Contribution à l'étude théorique et numérique de la rupture ductile des métaux, PhD thesis, Ecole Polytechnique, Palaiseau, France, 1992.

[14] Z.L. Zhang, E. Niemi, Analyzing ductile fracture using dual dilational constitutive equations, Fatigue Fract. Engrg. Mater. Struct. 17 (1994) 695–707.

[15] T. Pardoen, J.W. Hutchinson, An extended model for void growth and coalescence, J. Mech. Phys. Solids 48 (2000) 2467–2512.

[16] A. Benzerga, Micromechanics of coalescence in ductile fracture, J. Mech. Phys. Solids 50 (2002) 1331–1362.

[17] P.F. Thomason, Three-dimensional models for the plastic limit-loads at incipient failure of the intervoid matrix in ductile porous solids, Acta Metallurgica 33 (1985) 1079–1085.

[18] P.F. Thomason, A three-dimensional model for ductile fracture by the growth and coalescence of microvoids, Acta Metallurgica 33 (1985) 1087–1095.

[19] T. Pardoen, F. Scheyvaerts, private communication (2006).

[20] P. Suquet, Plasticité et homogénéisation, PhD thesis, Université Pierre et Marie Curie (Paris VI), France, 1982.

[21] G. Perrin, J.B. Leblond, Analytical study of a hollow sphere made of porous plastic material and subjected to hydrostatic tension—Application to some problems in ductile fracture of metals, Int. J. Plasticity 6 (1990) 677–699.

[22] Q.S. Nguyen, On the elastic plastic initial-boundary value problem and its numerical integration, Int. J. Numer. Meth. Engrg. 11 (1977) 817–832.